

Growth rate *versus* temperature relations characteristic of environmental stress cracks in low-density polyethylenes and the underlying thermodynamic mechanism

Yoshihito Ohde and Hiroshi Okamoto

Department of Engineering Sciences, Nagoya Institute of Technology, Gokiso-machi, Showa-ku, Nagoya 466, Japan

(Received 17 May 1982; revised 15 July 1982)

Growth rate *versus* temperature relations of environmental stress cracks (ESC) in low-density polyethylenes (PE) are investigated. In the experiments, bent PE specimens are immersed in dimethylsiloxanes (DMS) of various molecular sizes. The growth rates are increased from 10^{-9} to 10^{-4} m s⁻¹ by a few tens of degrees increase in temperature. The relations behave in apparently complicated manners depending on DMS molecular size, PE molecular weight and amount of bending deformation. Their Arrhenius type plots, however, fall into either of the two characteristic shapes as in PE ESC induced by several non-ionic surfactants and n-propanol. They are consistently interpreted in terms of the authors' thermodynamic theory. The active liquids, though incompatible with a stress-free polymer, migrate into its matrices in a restricted region at the crack tip. The change in the paths of the state shifts leading to failure in the relevant thermodynamic potential diagrams is essential to the ESC kinetics.

Keywords Environmental stress cracking; crack growth mechanism; irreversible thermodynamics; polyethylene; stress-induced swelling; crack growth kinetics

INTRODUCTION

In the presence of certain liquids (active liquids), crystalline olefin polymers often exhibit delayed and brittle-like failure when loaded at stresses below their strengths in air. The phenomenon is known as environmental stress cracking (ESC)¹. Amorphous glassy polymers exposed to organic liquids also exhibit a similar phenomenon².

The mechanisms of ESC have been studied in our laboratory by using polyethylenes (PE). Our earlier paper³ reported a method of measuring ESC growth rates in low-density PE specimens bent and immersed in active liquids. It enables us to study how ESC growth rate vs. temperature relations are affected by active liquids, PE molecular weight and amount of bending deformation. The Arrhenius type plots of the growth rates of PE ESC induced by a few non-ionic surfactants and n-propanol fall into either of the two typical shapes⁴. In two previous papers^{4,5} the processes of ESC growth were analysed in terms of irreversible thermodynamics. Active liquids, though incompatible with a stress-free polymer, become soluble with it if it is under a dilative stress field such as that in the region at a crack tip. The expected manner of the state shifts in the relevant thermodynamic potential diagrams and the breakdown concentrations introduced give a consistent interpretation of the experimental findings. The slopes of the Arrhenius type plots do not always give the activation enthalpies in these cases, because the front factor of the Arrhenius type equation is very temperature sensitive.*

In this paper, the growth rate vs. temperature relations of PE ESC induced by dimethylsiloxanes (DMS) are reported. DMSs are used as active liquids because their

compatibilities with PE change systematically with their molecular size. The effects of DMS molecular size, PE molecular weight and amount of bending deformation are discussed. The relations follow the theoretical predictions⁴ when reasonable adjustment of the parameter values are adopted.

The concept of the stress-induced swelling mechanism was first proposed by Gent⁶, and then by Brown⁷. The enhanced compatibility between PE and methanol induced by stress was reported by Soni *et al.*⁸ An ESC mechanism noting the surface energy reduction effects caused by active liquids was proposed^{9,10}. The last effect, however, appears irrelevant to the PE ESC studied here⁴.

EXPERIMENTAL

Materials

Three low-density PEs of different molecular weights (A, B and C) were used (*Table 1*).

A series of DMSs, the kinematic viscosities of which ranged from 2 to 10⁴ cSt (10^{-6} m² s⁻¹), were used as active liquids. Unless otherwise noted, they were used as received. Fractionation of 10³ cSt DMS was performed to check its low molecular weight components. First, an ethanol solution of 5% 10³ cSt DMS was prepared at 60°C. Then it was cooled to and held stationary at 30°C for 12 h. The upper diluted phase was sucked out, and the concentrated phase was again diluted with the same amount of ethanol. This was repeated four times. The fraction obtained was dried in vacuum at 170°C for 12 h.

Occasionally, non-ionic surfactants, nonylphenyl-

* The discussion of activation enthalpies in our earlier paper³ should be altered in this context.

Table 1 Specification of polyethylenes^a

PE ^a	Melt index (10 ⁻⁵ kg s ⁻¹)(10 ³ kg m ⁻³)	Density (10 ³ kg m ⁻³)	Yield strength (MN m ⁻²)	Molecular weight ^b
A	3.33	0.918	8.8	32 000
B	0.67	0.920	10.8	45 000
C	0.17	0.920	10.8	55 000

^a Manufactured by Mitsubishi Petrochemical Co.

^b Molecular weights were estimated through viscosity measurements of *p*-xylene solutions at 345K by using the relation¹⁴, $[\eta]$ (dl g⁻¹) = 1.05 × 10⁻³M^{0.63}

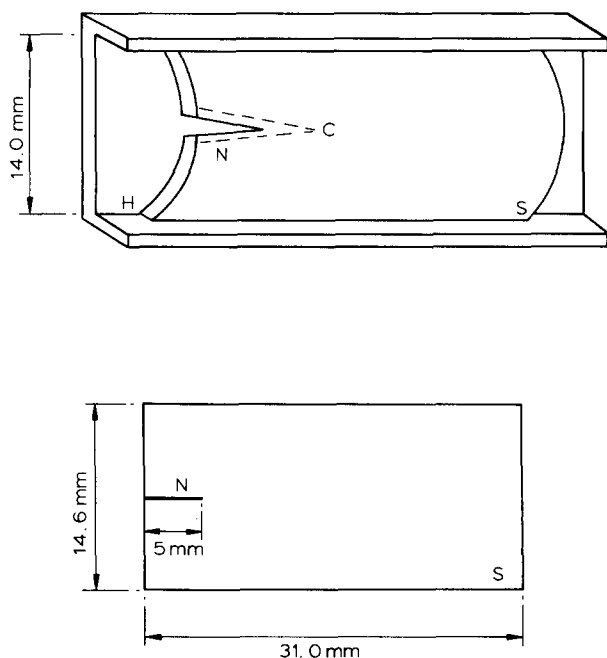


Figure 1 Experimental arrangement. Notched specimens (S) of a specified size, 31.0 × 14.6 × *D* (*D* = 0.43–0.90) mm were bent and set in holders (H) with a constant width of 14.0 mm. The length of the cut-in notch (N) was 5 mm. A linear crack (C) grew at the notch tip and its growth rates were measured

poly(oxyethylene) ethers were used. Their commercial names are NS206, NS210 and NS215 (Nippon Oil & Fats Co.), the last two digits of which denote the numbers of the oxyethylene group in the molecules.

Method

Our method was a version of constant deformation ESC. The procedures reported earlier³ were generally followed, but a few modifications were introduced to extend the range of the measurements. The measurements were made up to 85°C so as to cover the second relaxation of the growth rate increase⁴.

Procedures

Crack initiation (CI) treatment. Rectangular specimens of a specified size were bent and set in holders with a constant width (Figure 1). The bent specimens, notched by a razor, were first immersed in 20% NS210 aqueous solution, which was very active, at a certain temperature (CI temperature). A crack initiated at the notch tip, and grew straight along the ridge of the bent specimen. After a

certain time interval (CI time interval), the crack-initiated specimens, still in their holders, were washed with water and then acetone.

Growth rate measurements. They were then transferred into the active liquids in which growth rates were to be measured. In general, the crack grew on straight without branching. The increments of crack length were measured with a travelling microscope after appropriate time intervals, and converted to growth rates. The crack length measurements were made in air.

Modifications

(a) The specimens were annealed in this experiment at 90°C for 100 min. The CI temperatures for PE-A, B and C were chosen as 25°, 35° and 45°C respectively. Specimen thickness, *D*, covered the range from 0.43 to 0.90 mm. Unless otherwise noted, a standard size of 31.0 × 14.6 × 0.55 (±0.02) mm was used. The respective CI time intervals were 2 h for specimens of *D* = 0.43 mm, 1 h for those of *D* = 0.55 mm and 0.5 h for those of *D* = 0.90 mm. By these treatments, single cracks were initiated in 90% or more of the specimens. The differences in the CI temperatures and time intervals had no appreciable effect on the shapes of the Arrhenius type plots of their growth rates.

(b) Growth rates observed at a crack length of 15 mm were recorded conventionally as the data representing the respective experimental conditions.

Growth rates varied, more or less, during crack traverses through the specimens. With 10³ cSt DMS, the growth rates in PE-A and B ESC remained constant during the traverses, and those in PE-C ESC increased slightly. In contrast, with 20 cSt DMS, they decreased sharply at first and reached a stationary value (Figure 2). Fortunately, these variations were smaller than those caused by temperature changes.

The initial growth rate decreases were common to ESC induced by active liquids which were relatively less incompatible with PE. DMSs 2–30 cSt and NS206 were examples. The smaller the molecular size of DMS, the sharper the decrease. DMSs with larger molecular sizes did not cause this effect.

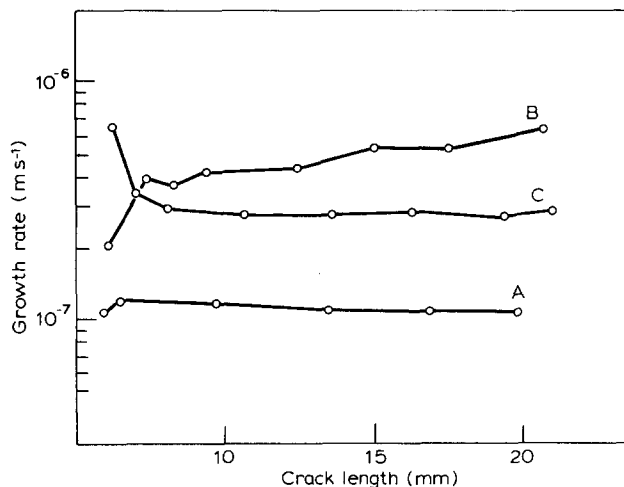


Figure 2 Three typical variations of ESC growth rates during crack traverses through the specimens: curve A, PE-B ESC induced by 10³ cSt DMS at 35°C; B, PE-C ESC, 10³ cSt DMS, 65°C; C, PE-B ESC, 20 cSt DMS, 50°C

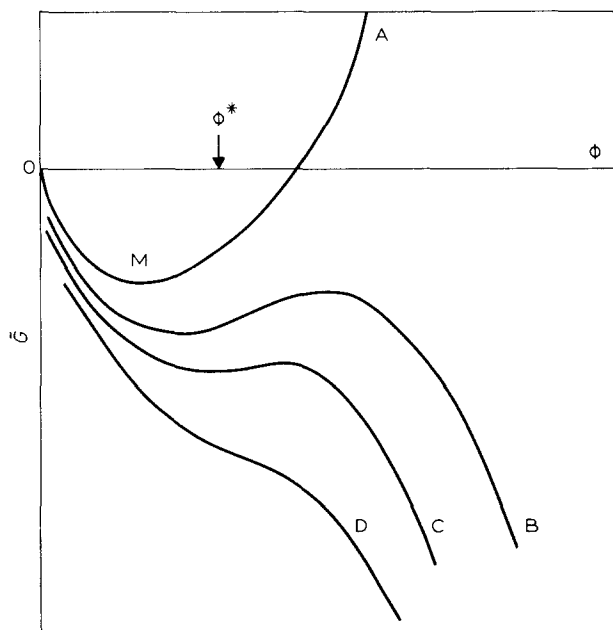


Figure 3 Schematic changes in the thermodynamic potential, G , versus liquid concentration, ϕ , in the crack tip region. The curves are labelled A–D in increasing order of the dilative stress parameter, Δp . A breakdown concentration, ϕ^* , is given in the Figure

The growth rate at each condition was measured by using 8–16 specimens. Though the scatter from specimen to specimen was rather large, the shapes of the Arrhenius type plots were clear.

THERMODYNAMIC THEORY OF ESC IN POLYMERS^{4,5}

Active liquid molecules migrate into polymer matrices in a restricted region at the crack tip under a dilative stress field due to stress concentration. Let the crack tip region be composed of n_r polymer molecules (r -mer) and n_s active liquid molecules (s -mer). The rates of the processes are governed by the relevant thermodynamic potential, G . Its reduced form,*

$$\tilde{G} = G/kTrn_r$$

is given by the Flory–Huggins approximation as

$$\tilde{G}(\phi; r, s, \chi, \Delta p) = \frac{1}{r} \ln(1 - \phi) + \frac{1}{s} \frac{\phi}{(1 - \phi)} \ln \phi + \chi \phi - \frac{\Delta p \phi}{1 - \phi}$$

where $\phi = sn_s/(rn_r + sn_s)$ is the volume fraction of the s -mers, χ is the interaction parameter between a segment of the polymer molecule and that of the active liquid molecule, which is inversely proportional to the absolute temperature, T , and Δp is the dilative stress parameter defined as $\Delta p = \Delta\sigma V/RT$, $\Delta\sigma$ being the dilative stress at the crack tip region subtracted by that of the contacting s -mer liquid phase, and V the molar volume of the segment. In the formulation, the ESC processes in PE are simply assumed to be confined to the amorphous phase⁴.

* The adoption of \tilde{G} instead of G is to separate the crack tip size effect.

Figure 3 shows the changes in the \tilde{G} vs. ϕ curves by increasing Δp . Similar changes are yielded by decreasing χ (or increasing T). Let us consider that, just after bending, the state of the crack tip region is at the origin, $\phi = 0$. It then shifts to the point M at $\phi = \phi_{\min}$ where the potential is a minimum. The theory introduces the breakdown concentration, ϕ^* , at which the region breaks due to weakening by local swelling. When ϕ_{\min} is less than ϕ^* (curve A), the region is stabilized at ϕ_{\min} and endures mechanically. By the increase in Δp or T , ϕ_{\min} approaches ϕ^* (curves B and C) from the left. Thermal fluctuation may allow the region to reach the state ϕ^* . This rarely occurs at first, but the likelihood is sharply enhanced when $\phi_{\min} \simeq \phi^*$. ESC will grow steadily through the repetition of the processes when ϕ^* is in the range from zero to ϕ_{\min} .

The curve D has no inflection point and decreases monotonically. The critical condition where the inflection point disappears is specified by critical parameters such as critical dilative stress, Δp_c , critical temperature, T_c , and the concentration at the inflection point, ϕ_c . Above the critical condition, $\Delta p > \Delta p_c$ or $T > T_c$, the vanishing of the inflection point allows state shifts towards $\phi = 1$. Another path along which it is easier to go to failure may be released. The breakdown concentration in this case is denoted by ϕ^{**} . A sudden increase in the growth rate will occur at the critical condition.

The two-stage increase in growth rates with increase in T , each stage of which consists of a sharp growth rate increase and its following relaxation, is expected if the critical temperature is in the experimental range and ϕ^* is less than ϕ_c . The single-stage increase in which there is no second sharp increase is expected when the critical condition is not attained in the experiment. It is also expected when ϕ^* is larger than ϕ_c .

The shapes of the \tilde{G} curves and the values of the breakdown concentrations play the primary roles in the growth kinetics of ESC. Estimations of the values of the parameters are difficult tasks and were performed so that the theory accommodated itself to the ESC phenomena observed. The values so estimated were in reasonable ranges, suggesting that the estimations were a satisfactory beginning.

RESULTS

DMS molecular size effects

Figure 4 shows growth rate vs. temperature relations of PE-B ESC induced by some DMS's having kinematic viscosities of 2–10⁴ cSt. Let us call the temperature, at which ESC growth begins, the growth temperature.

The plots obtained with DMSs having 50 cSt or higher viscosities had a common feature, namely the growth temperatures were lower. With increase in temperature, the growth rate increased very sharply in the low temperature range. A relaxation of the increase followed in the medium temperature range. At high temperature, a second sharp increase appeared and its relaxation followed. Our previous paper⁴ reported two-stage increases like these, and named them type 1.

The plots obtained with DMSs having 20 cSt or lower viscosities had another common feature, namely the growth temperatures were higher. The increase in temperature resulted in a very sharp increase in the growth rates. At a higher temperature, relaxation behaviour was observed with 20 cSt DMS. The relaxation

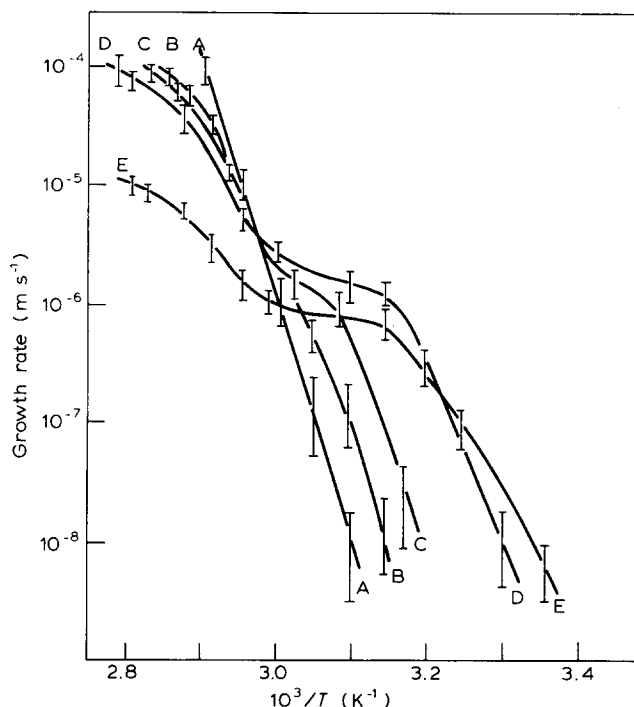


Figure 4 Growth rate versus temperature relations of PE-B ESC induced by DMSs of different molecular size, the kinematic viscosities of which are respectively: A, 2 cSt; B, 20 cSt; C, 30 cSt; D, 50 cSt; and E, 10⁴ cSt

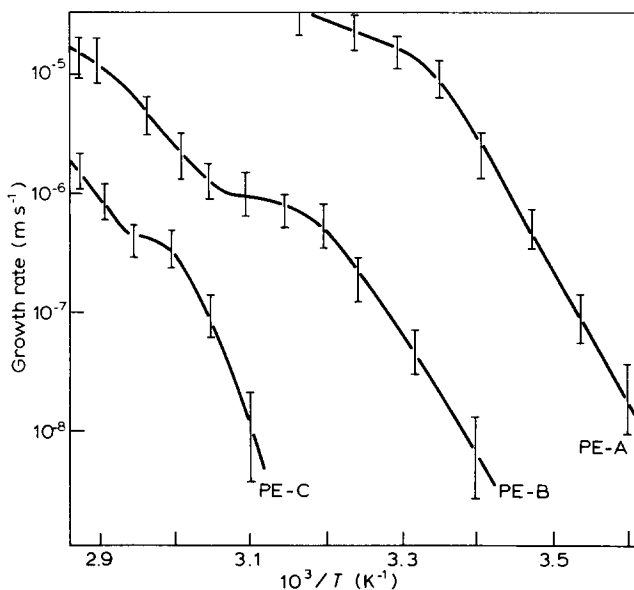


Figure 5 Growth rate versus temperature relations of ESC induced by 10³ cSt DMS in low-density PEs (PE-A, B and C) of different molecular weights

behaviour with 2 cSt DMS seemed beyond the measurable range. There was no second increase. We⁴ named single-stage increases like these type 2.

The plot with 30 cSt DMS exhibited an intermediate shape. It was barely type 1, but its first relaxation region was narrow, and its growth temperature was not low.

PE molecular weight effects

Figure 5 shows Arrhenius type plots of ESC growth rates in PE-A, B and C induced by 10³ cSt DMS. The PE

molecular weight effects were remarkable like the trends in our earlier paper⁴. The larger the PE molecular weights, the higher the growth temperatures. The values of growth rates decreased by two or more decades at a temperature in the low and medium temperature ranges. Their shapes were type 1. In PE-A, the high temperature behaviour seemed outside the measurable range. The shape of PE-B plot was typical. In PE-C, the growth temperature became higher, and the type 1 shape was poorly developed.

Figure 6 shows the effects in another way. The plot of PE-B ESC induced by 50 cSt DMS was type 1 (Figure 4), whereas the plot of PE-C ESC with the same liquid was type 2. However, the overall trends in the DMS molecular size effects were common to both the PEs.

Effects of the bending condition

Figure 7 shows the effects of changing specimen thickness on the Arrhenius type plots of PE-B ESC induced by 30 and 10⁴ cSt DMS.

With the decrease in specimen thickness or amount of bending deformation, the shapes of the plots changed from type 1 to type 2, and the growth temperatures became higher. The trends were confirmed by PE-B ESC induced by 20 and 10³ cSt DMS.

In ESC with 20 cSt DMS, the shape change occurred between the thicknesses of 0.60 and 0.70 mm. With 30 cSt DMS, it occurred by changing *D* from 0.43 to 0.55 mm (Figure 7). The larger the molecular size of DMS the milder bending condition at which the shape change occurred. In using the same thickness specimens, the type 1 shape was always better developed with 10⁴ cSt DMS than with 10³ cSt one.

It is noteworthy that the plots in the Figure 7 share the common features shown in Figures 4–6.

DISCUSSIONS

Comparison of the results with those in the earlier paper⁴

Figure 8 shows the \tilde{G} vs. ϕ curves calculated by setting $r = 10^3$, $\Delta p = 0.1$, $\chi = 0.5$ and $s = 5$ (corresponding to 2 cSt

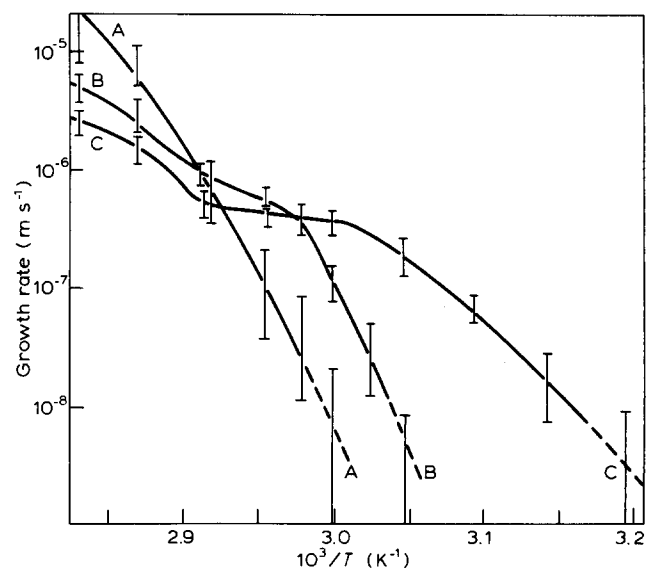


Figure 6 Growth rate versus temperature relations of PE-C ESC induced by DMSs having the kinematic viscosities A, 50 cSt; B, 10² cSt; and C, 10⁴ cSt

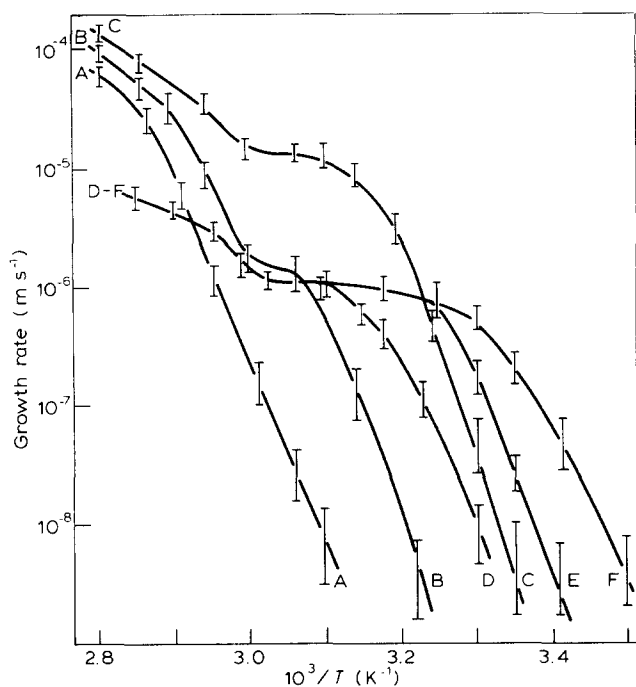


Figure 7 Effects of specimen thickness on growth rate versus temperature relations of PE-B ESC induced by 30 cSt DMS (curves A–C), and by 10^4 cSt DMS (curves D–F). The specimen thicknesses are A, 0.43; B, 0.55; C, 0.90; D, 0.43; E, 0.55; and F, 0.90 mm

DMS) and 50 (corresponding to 50 cSt DMS). The values of the χ parameters were estimated through

$$\chi = V(\delta_r - \delta_s)^2 / RT$$

where the solubility parameters, δ , were calculated by Small's method¹¹. The two χ values are practically equal. As in the examinations of PE ESC induced by NS210, NS215 and n-propanol⁴, the values of Δp and ϕ^* were assumed as 0.1 and 0.1 respectively. According to the theory, we cannot expect from the \tilde{G} curve in Figure 8 that ESC might be induced by larger size DMSs, because its ϕ_{\min} is very close to zero.

The authors at first suspected that the ESC by poly-DMSs were induced by oligomers which might be in the commercial grades. However, fractionation of 10^3 cSt DMS, described in the experimental section, brought no change in the ESC data. In addition, the experiment of PE-B ESC induced by mixtures of 10^3 and 2 cSt DMSs showed that the increase in the latter fraction brought a gradual shape change from type 1 (with pure 10^3 cSt DMS) to type 2 (with pure 2 cSt DMS). It is clear that the poly-DMSs used do not contain enough oligomer to affect the plots.

It may be suggested that poly-DMS works in other ways than oligo-DMS. However, as has been repeatedly described, there is no essential difference in the growth rate vs. temperature behaviours observed by poly-DMSs and other active liquids including oligo-DMSs and NS surfactants. Table 2 shows the shapes of the Arrhenius type plots of the ESC growth rates observed in this work and earlier⁴. Note that NS206, which is the least incompatible with PE among the three NS surfactants, caused the type 2 plot like oligo-DMSs. The tendencies that the type 1 plots are found in ESC by using lower

molecular weight PEs, more incompatible active liquids and severer bending conditions prevail among the active liquids examined. This suggests that all the active liquids play the same role in the ESC mechanisms.

Interpretations by the proposed theory

The χ parameters relevant to poly-DMS often depend on polymer concentrations. Sugamiya *et al.*¹² said that the χ parameter values in the n-alkane–poly-DMS system varied with polymer concentration as $\chi = 0.4 + 0.2\phi$. Flory *et al.*¹³ reported that $\chi = 0.5 + 0.3\phi$ in the benzene–poly-DMS system. Concurrently, we introduce a similar dependence in our χ parameter values. A larger dependence may be allowed, since the pairs in our cases are incompatible in a stress-free state.

The values of the dilative stress at the crack tip may be varied by the active liquid used. The active liquids which are more incompatible like poly-DMSs will allow larger values of Δp than will the NS surfactants on n-propanol.

Figure 9 shows the \tilde{G} curves recalculated using a concentration-dependent χ parameter, $\chi = 0.4 + 0.5\phi$, and several Δp values around 0.375 for the pair $r = 10^3$ and $s = 50$. For a range of Δp values, the values of ϕ_{\min} are in a reasonable range to induce ESC failure. The shapes of the \tilde{G} curves are insensitive to s parameters larger than 50. The figure shows an applicability of the theory to the ESC induced by poly-DMSs by using reasonable adjustments of the values of χ and Δp . The adjustments are somewhat artificial, but no basic modifications are introduced into the scheme of the theory.

Variations of Δp and ϕ^* with specimen thicknesses

Let us call the temperature at which the second sharp growth rate increase begins the transition temperature. According to our thermodynamic interpretation, it

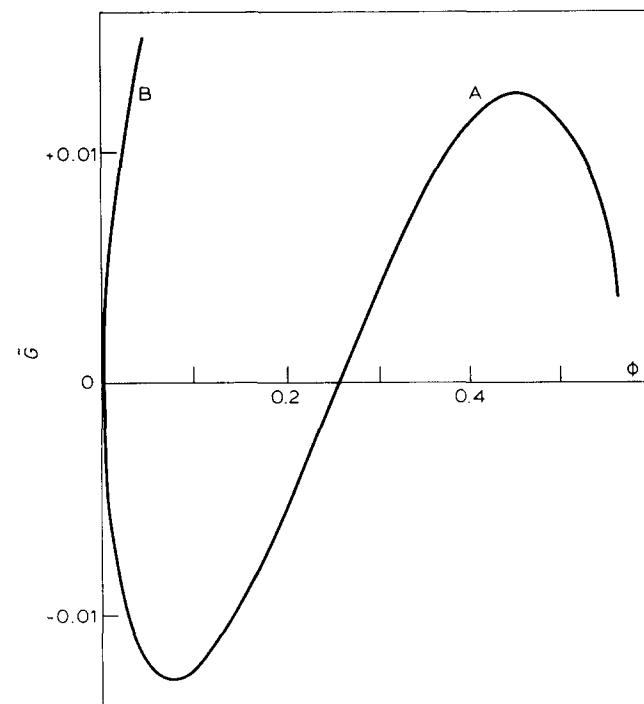


Figure 8 Thermodynamic potentials G versus ϕ , calculated by using parameters $r = 10^3$, $\chi = 0.5$, $\Delta p = 0.1$, and $s = 5$ (curve A) and $s = 50$ (curve B) respectively

Table 2 Shapes of the ESC growth rate vs. reciprocal temperature plots in low-density polyethylenes

	PE-A	PE-B	PE-B	PE-B	PE-C
	Specimen thickness (10^{-3} m)				
Active liquids	0.55	0.43	0.55	0.90	0.55
DMS 2 cSt	—	—	2	—	—
20 cSt	—	2	2	1	—
30 cSt	—	2	1	1	2
50 cSt	1	—	1	—	2
10^2 cSt	—	—	—	—	1
10^3 cSt	1	1	1	1	1
10^4 cSt	1	1	1	1	1
NS206	—	—	2	—	—
NS210 ^a	1	—	1	—	2
NS215	—	—	1	—	1
n-Propanol	2 ^b	—	2 ^b	—	2 ^b

^a The surfactant NS210 is nearly the same material known as Igepal CO630 or Antalox CO630

^b The situation in which the type 2 shape is exhibited by n-propanol is different from those in which it is exhibited by DMSs and NS surfactants. See text.

corresponds to the critical temperature, T_c . Because the transition temperatures by 10^4 cSt DMS (Figure 7) were unchanged by variations in specimen thickness, the values of Δp seem constant irrespective of the amounts of bending deformation. The transition temperatures with 30 cSt DMS behaved similarly. The constancy in Δp is natural because the crack tip region is in a yielded state. The stress levels, however, will change according to the compatibilities of the active liquids used, as suggested in the preceding section. The decrease in the elastic energy stored in the bodies of thinner specimens will result in higher breakdown concentrations and higher growth temperatures. When ϕ^* exceeds ϕ_c , the growth rates will exhibit a single-stage behaviour, which is type 2. The expected tendencies are seen in Figure 7.

The lowering in the stored elastic energy and the resulting increase in the breakdown concentrations may be brought about by less incompatible active liquids like those yielding the initial growth rate decreasing phenomenon in Figure 2. By using DMSs of smaller molecular sizes, the growth temperatures will become higher, and the shapes will change from type 1 to type 2. The expected tendencies are confirmed by Figures 4 and 6.

The data in Figure 5 are attributable to the increase in the breakdown concentrations with the increase in PE molecular weight, as pointed out earlier⁴.

The type 2 plots can be observed in the two situations. The type 2 plots in Figures 4, 6 and 7 may be due to the situations of $\phi_c \leq \phi^*$. The plots of ESC induced by n-propanol were apparently of type 2. But the situations should be attributed to the critical temperature in those cases being beyond the experimental range⁴.

At present, we consider that the parameters Δp and ϕ^* (and ϕ^{**}) vary according to the compatibilities between PE and active liquid pairs. The variations may be partly inherent in the constant deformation method used here.

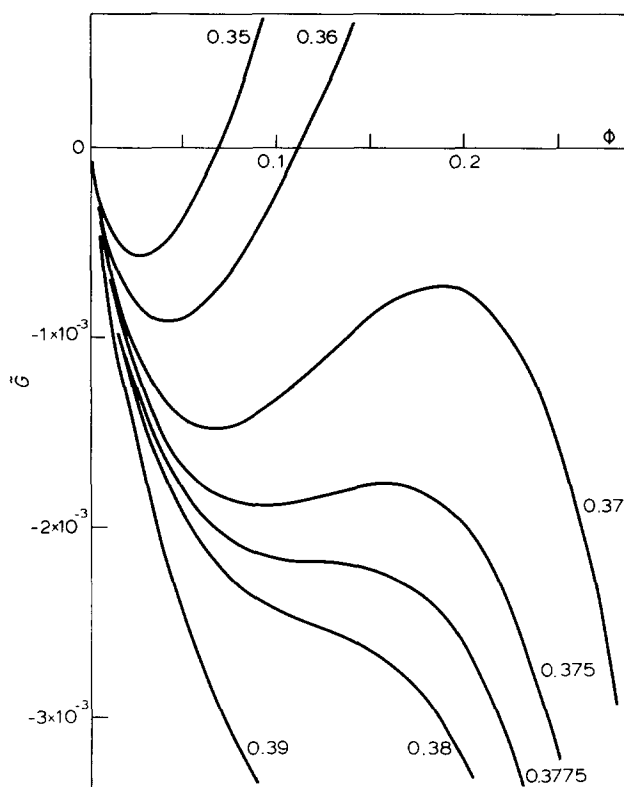


Figure 9 Thermodynamic potentials G versus ϕ , calculated using a concentration-dependent interaction parameter $\chi = 0.4 + 0.5\phi$, and several Δp around 0.375, of the pair of $r = 10^3$ and $s = 50$. The values of Δp are indicated in the Figure

ACKNOWLEDGEMENTS

The authors are grateful to Mitsubishi Petrochemical Co. and Nippon Oil & Fats Co. for their presentations of materials. The authors thank Mr Y. Nagata for his help in the preparation of specimens. Part of this study was supported financially by the Grant-in Aid for Developmental Scientific Research by the Japanese Ministry of Education, Science and Culture in 1981.

REFERENCES

- Howard, J. B. 'Crystalline Olefin Polymers', Part II (Eds. R. V. A. Raff and K. W. Doak), Wiley-Interscience, New York, 1964, p. 47
- Kramer, E. J. 'Developments in Polymer Fracture' vol. 1 (Ed. E. H. Andrews), Applied Science, London, 1979, p. 55
- Ohde, Y. and Okamoto, H. *J. Mater. Sci.* 1980, **15**, 1539
- Okamoto, H. and Ohde, Y. *Polymer* 1982, **23**, 1204
- Okamoto, H. and Ohde, Y. *Polymer* 1980, **21**, 859
- Gent, A. N. *J. Mater. Sci.* 1970, **5**, 925
- Brown, H. R. *Polymer* 1978, **19**, 1186
- Soni, P. L. and Geil, P. H. *J. Appl. Polym. Sci.* 1979, **23**, 1167
- Andrews, E. H. and Bevan, L. *Polymer* 1972, **13**, 337
- Haward, R. N. and Owen, D. R. *J. Proc. R. Soc. Lond. A* 1978, **352**, 265
- Burrell, H. 'Polymer Handbook' (Eds. J. Brandrup and E. H. Immergut), Wiley-Interscience, New York, 1975, IV-337
- Sugamiya, K., Kuwahara, N. and Kaneko, M. *Macromolecules* 1974, **7**, 66
- Flory, P. J. and Shih, H. *Macromolecules* 1972, **5**, 761
- Tremontozzi, Q. A. *J. Polym. Sci.* 1957, **23**, 887